Article

Cell Reports

Neuronal Responses to Conspecifics in the Ventral CA1

Graphical Abstract

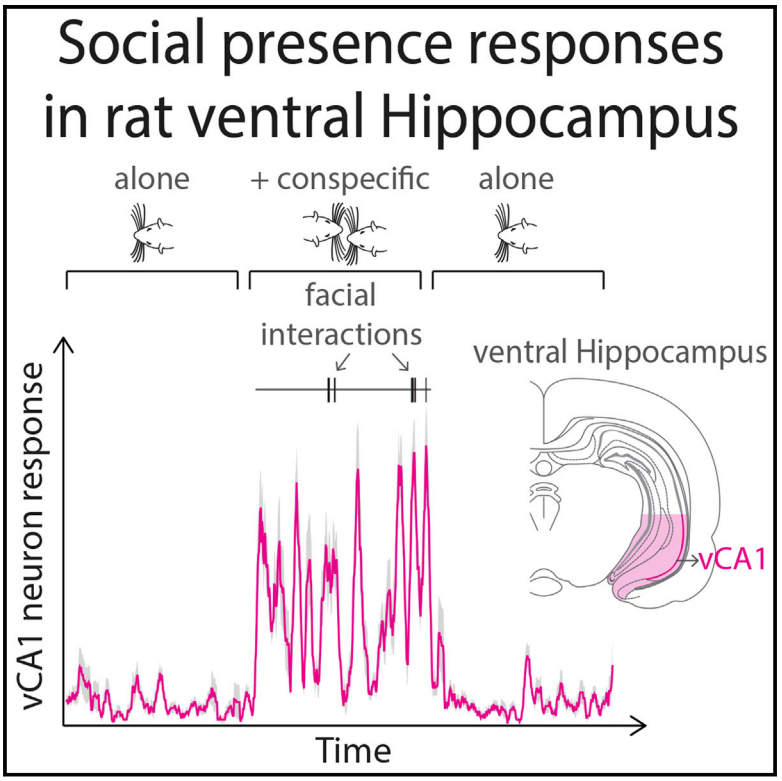

Authors

Rajnish P. Rao, Moritz von Heimendahl, Viktor Bahr, Michael Brecht

Correspondence

rajnish.rao@bccn-berlin.de (R.P.R.), michael.brecht@bccn-berlin.de (M.B.)

In Brief

Rao et al. report large firing rate modulations in ventral CA1 due to the presence of conspecifics. Discharges in ventral CA1 varied with sex and identity of the conspecific and were distinct from those observed in dorsal CA1.

Highlights

- Ventral CA1 neurons respond to the presence of conspecifics
- Response modulation is dependent on the sex and the individual presented
- Ventral CA1 neurons show little or no response to object presence
- Ventral CA1 responses are distinct from those of dorsal CA1

Rao et al., 2019, Cell Reports *27*, 3460–3472
June 18, 2019
https://doi.org/10.1016/j.celrep.2019.05.081

CellPress

OPEN ACCESS
CellPress

Cell Reports
Article

Neuronal Responses to Conspecifics in the Ventral CA1

Rajnish P. Rao,[1,*] Moritz von Heimendahl,[1,2] Viktor Bahr,[1] and Michael Brecht[1,3,*]
[1]Bernstein Center for Computational Neuroscience Berlin, Humboldt University of Berlin, Philippstrasse 13 Haus 6, Berlin 10115, Germany
[2]Present address: Boehringer Ingelheim Pharma GmbH & Co. KG, CNS Diseases, Biberach an der Riss, Germany
[3]Lead Contact
*Correspondence: rajnish.rao@bccn-berlin.de (R.P.R.), michael.brecht@bccn-berlin.de (M.B.)
https://doi.org/10.1016/j.celrep.2019.05.081

SUMMARY

Conspecific recognition and discrimination is a vital aspect of social interactions. Genetic manipulations have implicated the CA2 sub-field and ventral hippocampus in rodent social memory. However, little is known about the nature of hippocampal responses to social signals. We characterized ventral CA1 responses in rats while interacting with conspecifics across a gap. Many cells showed unusual "social presence responses," i.e., large elevations of firing rates, which were contingent on the presence of a conspecific. Sharp-wave ripple activity was also increased by conspecific presence. The cells were modulated by facial touch and ultrasonic vocalizations. In male rats, female conspecifics evoked stronger responses than males. In addition, responses to females differed more strongly between individual females than between males. Cells showed little response to object presence. Ventral CA1 responses were also markedly different from those of dorsal CA1, where most cells were weakly inhibited by conspecific presence.

INTRODUCTION

Rats live in large social groups and display a wide range of interactions with their conspecifics. Complex social interactions can be observed during the display of dominance hierarchies, mating, and parental behaviors (Barnett, 1958; Scott, 1966). The ability to recognize and distinguish between different individuals (e.g., a potential mating partner or a competitor for resources and/or mates) in these contexts is vital. Several studies have shown that rodents can discriminate between conspecifics (Husted and McKenna, 1966; Petrulis, 2009; Thor and Holloway, 1982). They are capable of matching an individual with its olfactory signature (Gheusi et al., 1997; Johnston and Jernigan, 1994; Petrulis, 2009; Popik et al., 1991; Sawyer et al., 1984), and there are indications that ultrasonic vocalizations in female mice are individual specific (Moles et al., 2007). These observations suggest that, at the neuronal level, there is an integrated representation for conspecifics that relies on information from more than one sensory modality (Johnston and Jernigan, 1994).

In addition to the involvement of primary sensory areas, a detailed description of the role of hypothalamic structures in parental (Dulac et al., 2014) and aggressive behaviors (Anderson, 2016) is available. However, we have little information about the role of forebrain structures. This particularly applies to the hippocampus, which receives integrated input from most sensory cortices (Burwell, 2000) and therefore is an ideal candidate for the integrated representation of conspecifics. Studies on patients with hippocampal lesions (Scoville and Milner, 1957; Zola-Morgan et al., 1986) provided the first lines of evidence to this theory. Subsequently, direct electrophysiological evidence from humans (Quiroga et al., 2005) and monkeys (Sliwa et al., 2016) has demonstrated the higher-order representation of social signals in the hippocampus. These studies have established the existence of the so-called concept cells (Quiroga, 2012), which respond to a particular individual (and other complex stimuli) in a distinctly multimodal fashion (i.e., to pictures, name strings visually presented, name strings played back; Quian Quiroga et al., 2009).

There are however conflicting reports with regard to social representations in the rodent hippocampus, especially from lesion studies. While some have implicated a role for the hippocampus in recognition memory (Kogan et al., 2000; Uekita and Okanoya, 2011), other have provided contrary evidence (Bannerman et al., 2001; Feinberg et al., 2012; Petrulis and Eichenbaum, 2003; Squires et al., 2006). It also appears that an intact hippocampus is required for recollection memory in hamsters (Lai et al., 2005). Hippocampal lesions affect social behaviors (Sams-Dodd et al., 1997), but again, there is evidence to the contrary (Becker et al., 1999; Daenen et al., 2002). Further, using direct electrophysiological recordings, it was demonstrated that the CA1 was only weakly modulated by the presence of other rats (Alexander et al., 2016; von Heimendahl et al., 2012; Zynyuk et al., 2012). However, it is important to note that all these reports focused on the dorsal pole of the hippocampus.

At the anatomical level, the cortical and subcortical connections of the dorsal and ventral hippocampus are very different (Strange et al., 2014). This led to the suggestion that the hippocampus is functionally segmented along its dorsoventral axis; with the ventral part (corresponding to primate anterior hippocampus) involved in functions that are qualitatively different from and independent of the dorsal end (Moser and Moser, 1998). Several lines of evidence have subsequently led to the suggestion that the dorsal hippocampus is involved in cognitive functions devoid of emotional content (such as spatial navigation) while the ventral pole plays a role in emotion and stress

regulation (i.e., affective disorders; Fanselow and Dong, 2010). Paralleling the connectivity differences along the dorsoventral axis, the precision of spatial representation declines toward the ventral pole (Jung et al., 1994; Kjelstrup et al., 2008; Maurer et al., 2005; Poucet et al., 1994; Royer et al., 2010) and potentially allows for the representation of non-spatial information (Royer et al., 2010). Despite this, the ventral population encodes a distributed representation of space and preserves spatial coding to a degree comparable to dorsal populations (Keinath et al., 2014). Taken together, these findings would suggest that social signals in the rodent brain are not likely to be encoded by the dorsal hippocampus. In a seminal paper using genetic manipulations, it was shown that the CA2 sub-field is essential for social memory (Hitti and Siegelbaum, 2014). CA2 activity is required for encoding, consolidation, and recall phases of social memory (Meira et al., 2018), and stimulation of the CA2 area enhances social recognition memory (Smith et al., 2016). Subsequently, it was demonstrated that optogenetically shutting down ventral CA1 (vCA1) but not dorsal CA1 (dCA1) impaired social recognition memory (Okuyama et al., 2016). The vCA1 neurons and their projections to the nucleus accumbens (NAc) shell constitute the site of social memory storage (Okuyama et al., 2016). Also, the vCA1 receives direct excitatory inputs from the socially responsive CA2 sub-field (Meira et al., 2018). Genetic and pharmacological disruption of glutamatergic synaptic transmission has shown that the ventral (but not dorsal) CA3 is required for the encoding of social memory (Chiang et al., 2018). In addition, neuropeptide-mediated signaling mechanisms involved in regulation of social behaviors operate in the CA2 and CA3 hippocampal sub-fields (Lin et al., 2018; Raam et al., 2017; Smith et al., 2016).

In this investigation, we were interested in understanding the nature of neuronal responses to conspecifics in the ventral hippocampus. The following key questions were asked: (1) Is the ventral hippocampus responsive to familiar conspecifics? (2) How do these responses relate to the encoding of spatial information? (3) How are hippocampal rhythms involved in memory processing modulated by the presence of familiar conspecifics? (4) Is the ventral hippocampus modulated by multisensory inputs that are exchanged during interactions between conspecifics? (5) Is the ventral hippocampus capable of sex and individual discrimination? (6) Are the responses to conspecifics distinct from responses to object controls? (7) How do the ventral hippocampal responses to conspecifics differ from those in the dorsal hippocampus?

RESULTS

In this study, we used the gap paradigm that consists of two elevated platforms separated by a gap (Figure 1A). Rats spontaneously reach out across the gap and perform facial interactions (Figure S1A; Wolfe et al., 2011). The subject rats (male Wistars) were presented with stimuli that were either conspecifics (age-matched males and females) or object controls. To avoid confounds of novelty, the subject rats were familiarized to all stimuli during habituation to the experimental setup. On a typical experimental day, five to eight recording sessions were performed, during which stimuli were presented in a pseudorandom order. Each recording session consisted of three epochs: an initial baseline period (5 min), when the subject rat was present alone on the setup; a stimulus presentation epoch, during which facial interactions occurred (5 min); and an end baseline period (5 min), when the subject rat was again alone. We monitored the facial interactions by low- and high-speed videography. A total of 1,156 spontaneous facial interactions (as defined by whisker-to-whisker contacts; Figure S1A, top) were identified. These included 858 snout-to-snout contacts (Figure S1A, bottom). Ultrasonic vocalizations were recorded using specialized microphones placed below the platforms (Figure 1A). In a subset of experiments, repeated presentations of the same stimuli were performed, while in most others, multiple different stimuli were presented. We acquired neuronal responses from vCA1 (Figures 1B and S1B) of subject rats (n = 4). We used spike shape characteristics to classify the units as regular (n = 106) or fast spiking (n = 10; Figures S1C–S1F; see STAR Methods), and electrolytic lesions to identify recording sites (Figures 1B and S1G–S1K). Neuronal responses were analyzed over several time scales: from fast millisecond-precise whisker-to-neuron analysis to slower modulation by conspecific presence that occurred over several minutes. For comparison with dCA1 (Figure S1L), we reanalyzed data acquired in a previous study using a similar paradigm (von Heimendahl et al., 2012).

Ventral CA1 Neurons Are Modulated by Social Presence

We first analyzed the responses of vCA1 excitatory neurons to the presence of conspecifics at a time scale of minutes by plotting their firing rates as moving averages in each recording session (example unit shown in Figures 1C–1F). In the first two sessions, we presented a female (F1; Figure 1C) and a male conspecific (M1; Figure 1D). The firing rate of this unit was low during the initial and end baseline periods. However, there was a strong and sustained increase in the firing rate when the conspecific was present (indicated by gray horizontal line). We then performed repeat presentations of the same two stimuli during the third (Figure 1E) and fourth (Figure 1F) recording sessions. Again, consistent increases in firing rates were observed after the conspecific was introduced (spike rasters in Figure 1G, top) and only when the conspecifics were present. What is notable in all four sessions is that the modulations were not restricted to the facial interactions (indicated by red or blue vertical lines; Figures 1C–1F), suggesting that they were elicited by conspecific presence and not necessarily due to facial interactions. We also observed differential responses when different conspecifics (cf. Figures 1C and 1D) were presented.

In order to identify and classify vCA1 units in terms of the large-scale firing rate modulations, we used a z-score criterion (see STAR Methods). A unit was considered strongly modulated if its firing rate during conspecific presence was 4 SD above the subject-alone condition (i.e., a combination of initial and end baselines periods). We observed multiple instances during which the activity of the example unit (Figures 1C–1F) was above this criterion (indicated by dashed lines). Analysis of individual recording sessions showed that 54% of vCA1 units were strongly modulated by conspecific presence during at least one recording session. A smaller fraction (22%) showed weak responses (<4 but >3 z-scores) during at least one session, while

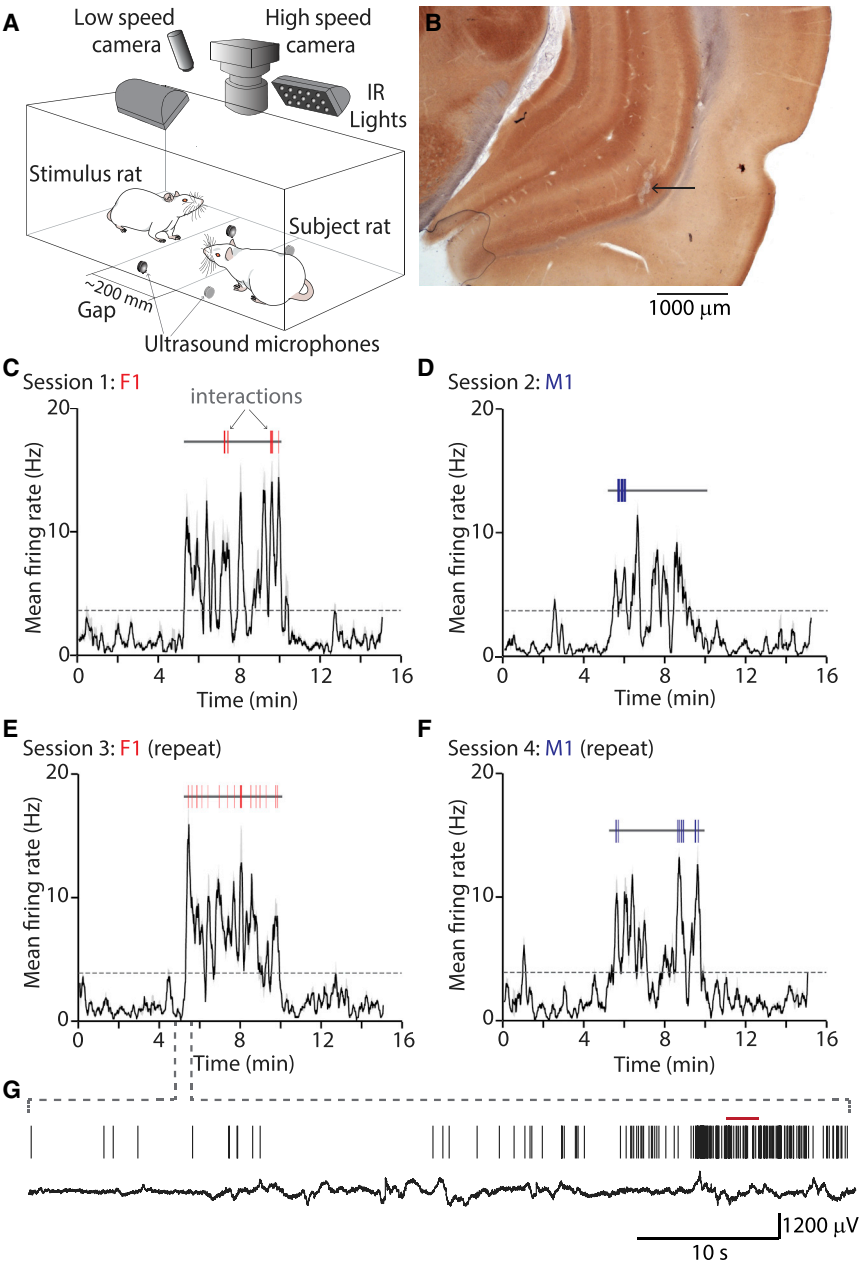

Figure 1. vCA1 Neurons Are Modulated by the Presence of Conspecifics

(A) Social interactions between conspecifics (subject and stimulus rats) were studied using a gap paradigm. Facial touch episodes were videographed by low- and high-speed cameras under infrared (IR) illumination, and ultrasonic vocalizations were recorded with specialized microphones.

(B) Photomicrograph of cytochrome oxidase stained coronal brain section (bregma: −5.64 mm) showing electrolytic lesions in *stratum pyramidale* of vCA1 (black arrow, scale bar: 1000 μm).

(C) Mean firing rate of an example vCA1 unit over the entire duration of recording session 1. Low firing rates were observed during the initial and end baseline periods (i.e., first and last 5-min epochs, when subject rat was alone). Large increases in firing rate were observed when a conspecific (F1) was introduced (during middle 5-min epoch, indicated by gray horizontal bar). Red vertical lines indicate time points where facial interactions with stimulus occurred. Dotted line indicates four z-score criteria for strong response to presence.

(D) Mean firing rate of the same unit during recording session 2, where a different conspecific (M1) was presented. Blue vertical lines indicate facial interactions with this stimulus rat.

(E) Mean firing rate of the same unit during recording session 3, where the presentation of conspecific F1 was repeated.

(F) Mean firing rate of the same unit during recording session 4, where the presentation of conspecific M1 was repeated.

(G) A zoom-in of the recording shown in (E) (30 s before and after onset of conspecific presence). Spike rasters (top) for the unit shown in (E) and raw LFP trace (below) at the recording site. A touch episode that occurred in this duration is indicated in red.

23% of units were not modulated. Modulation of average firing rates could possibly arise due to behavioral differences wherein the subject rat exhibits greater periods of inactivity during the baseline periods. Indeed, the running speed increased during conspecific presence (mean ± SD: 4.9 ± 0.78 cm/s) when compared to when it was alone (2.7 ± 0.91 cm/s). However, when we compared the firing rates of the vCA1 units with the running speeds of the subject rats, we observed little or no correlation at the level of individual recording sessions (Figures S2A–S2D) and the population (Figure S2E).

Another confound for our observations could arise from the spatial aspects of the gap paradigm. It could be argued that the modulations observed in vCA1 cells are a result of place cells firing in the gap. To investigate this, we tracked the positions of the subject rat to generate spatial firing maps. Spatial firing plots indicated that there was little or no spatially modulated activity when the subject rat was alone, despite making several head extensions over the gap (Figure S3A, for unit shown in Figures 1C–1F). When the stimuli were introduced, extensive firing (red dots) was seen in the area of interaction with the subject rat (gray trace; Figure S3B). Spatial correlation between the firing rates in subject-alone versus conspecific-present epochs were weak both at the level of the example unit ($r = 0.24$; cf. Figures S3A and S3B) and the population of vCA1 neurons analyzed (Figure S3C), indicating that the difference in average rate cannot be explained simply by a static place field and different occupancy maps. We also computed the spatial information content (Skaggs et al., 1992) and found it to be low in both subject-alone and conspecific-present epochs (Figure S3D), suggesting that the introduction of the conspecific does not lead to the appearance of a place field.

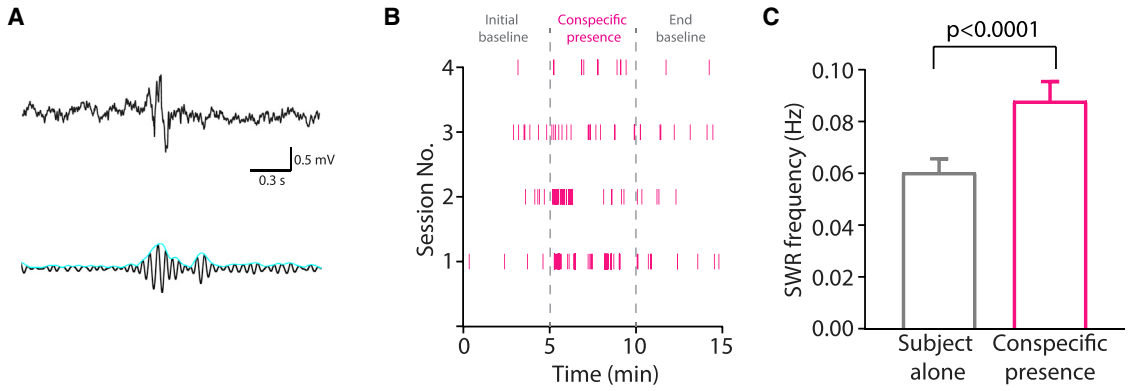

Figure 2. Modulation of Ventral Hippocampal SWRs by Conspecific Presence

(A) Representative example of SWRs (top, raw trace; bottom, filtered) recorded in the ventral hippocampus.

(B) Raster plot showing occurrence of SWRs during four recording sessions, with conspecific presence epochs demarcated by dotted lines.

(C) Population plot of SWR frequency in vCA1 in subject-alone and conspecific-present conditions (n = 100, $p < 0.0001$, Wilcoxon signed rank test).

Ventral Hippocampal Sharp-Wave Ripples (but Not Theta) Are Increased by Conspecific Presence

The dCA2-vCA1-NAc circuit has been suggested to form the basis of social memory (Hitti and Siegelbaum, 2014; Okuyama et al., 2016). We tested if sharp-wave ripples (SWRs) triggered by the CA2 subfield (Oliva et al., 2016) could also be observed in the ventral hippocampus and potentially contribute to the conspecific presence related increase in vCA1 firing rates. We analyzed the frequency of SWR events in the ventral hippocampus (Figure 2A). As shown in the example recording sessions, there was a marked increase in ripple activity due to conspecific presence (delineated by gray dotted lines; Figure 2B). This was also true across all of the ventral hippocampal recording sites ($p < 0.0001$; Figure 2C). The increased SWR activity during conspecific presence was not correlated with the running speed of the subject rat, suggesting that the increased ripple activity was not a consequence of increased immobility (Figure S4G).

To investigate the role of attentional mechanisms, we analyzed the modulation of hippocampal rhythms by conspecific presence. Introduction of a conspecific led to only a marginal increase in local field potential (LFP; raw trace in Figure 1G, bottom) power in the theta range (6–10 Hz), as shown in an example session (Figures S4A and S4B). This was also the case in all ventral hippocampus recording sites that we analyzed where there was a small, non-significant and generalized increase in LFP power due to conspecific presence when compared to the subject-alone condition (Figure S4C). Facial touch also did not lead to any modulation of LFP power, as shown in the example session (Figures S4D and S4E) and in the population (Figure S4F). Also, theta power in the ventral hippocampus was not correlated with the running speed of the subject rat (Figure S4H).

Ventral CA1 Neurons Are Modulated by Facial Touch and Stimulus Calls

Having observed the responses to presence, we next investigated the triggers for these changes at shorter time scales. Specifically, we asked if vCA1 responses to conspecific presence were related to the multi-modal signaling that is characteristic of facial interactions. Facial interactions in the gap paradigm are characterized by extensive whisker-to-whisker touch (Bobrov et al., 2014; Lenschow and Brecht, 2015; Wolfe et al., 2011) and ultrasonic vocalizations (Rao et al., 2014). We first aligned the spike trains of vCA1 neurons to the onset of whisker touch and generated peri-stimulus time histograms (PSTHs). Facial touch evoked both excitatory (Figure 3A) and inhibitory (Figure 3B) responses, as seen in the two example vCA1 units. Interestingly, these responses occurred over extended time scales (1200–1500 ms). A comparison of touch evoked versus baseline firing rates indicated that the overall vCA1 population was significantly inhibited by touch ($p = 0.0009$; Figure 3C). While a small fraction of units (11%) showed significant upregulation by facial touch at the individual level, the population effect was a result of nearly a third of vCA1 units (28%) being significantly inhibited by facial touch.

We next studied the responses of vCA1 neurons to ultrasonic calls. PSTHs were triggered to the onset of the calls. The calls in themselves were sorted according to the source. As seen in the example unit, there was no modulation by the subject rat's own calls (Figure 3D), while the stimulus rats' calls resulted in an inhibition (Figure 3E). Again, the time scale of these responses was delayed (200–250 ms). A population plot of the response indices also demonstrates the inhibition by stimulus calls ($p = 0.003$; Figure 3F).

In Males, Ventral CA1 Cells Respond More Strongly to Females Than to Males and Discriminate More Strongly between Females

Sex is a major determinant of social interaction patterns. Hence, we analyzed responses of vCA1 (recorded in male rats) as a function of the sex of the interaction partner. As shown in the example, responses to presence were often stronger to females than to males (Figures 4A and 4B, respectively). Comparison of each vCA1 unit's normalized firing rate for the presence of female versus male conspecifics revealed that responses to female presence were stronger in most cells ($p = 0.0124$; Figure 4C). The estrous state of female stimuli does not appear to be correlated to increased activity in vCA1 units due to female presence ($p = 0.6353$; Figure S5E).

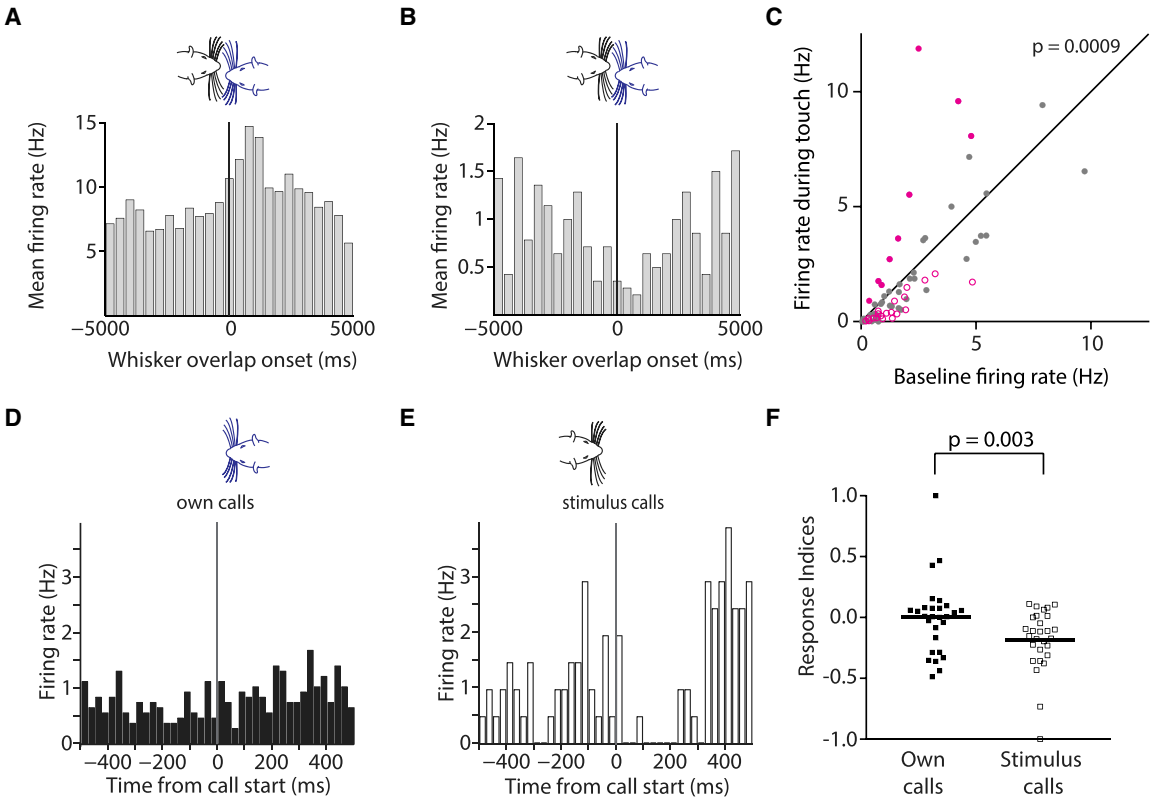

Figure 3. vCA1 Neurons Are Modulated by Facial Touch and Ultrasonic Vocalizations

(A) PSTH for an example vCA1 unit showing excitatory response when aligned to onset of whisker touch (bin size: 400 ms).

(B) PSTH for a different vCA1 unit showing inhibitory response when aligned to onset of whisker touch (bin size: 400 ms).

(C) Scatterplots comparing baseline firing rates of vCA1 units to firing rate during facial interactions with conspecifics. Permutation tests were used to classify units as being significantly excited (filled magenta circles), significantly inhibited (open magenta circles), or not modulated (filled gray circles). The population was significantly inhibited ($p = 0.0009$, $n = 82$, Wilcoxon signed rank test).

(D) PSTH for an example vCA1 unit aligned to the onset of subject rat's own calls (bin size: 25 ms).

(E) PSTH for vCA1 unit shown in (D) aligned to the onset of stimulus rats' calls (bin size: 25 ms).

(F) Comparison of response indices indicating a significant inhibition of vCA1 population by stimulus calls compared to subject's own calls ($p = 0.003$, $n = 28$, Wilcoxon signed rank test). Horizontal bars indicate the population median.

Further, it also appeared that several vCA1 units fired differently for different individuals. In order to avoid confounds of sex, we compared responses of every vCA1 unit to an individual within a given sex, i.e., one female versus another (or one male versus another). Comparison of normalized firing rates for the presence of one individual versus another showed that vCA1 units fire differentially for different individuals, in both females (Figure 4D) and males (Figure 4E). Interestingly, this difference is greater for females than for males, indicating that responses to females were more varied than responses to males. Indeed, firing rate differences (as determined by the distance from the unity line for data points on the scatterplot) for females are greater than for males ($p = 0.0294$; Figure 4F). This ability of vCA1 units to better discriminate between two females than two males could arise due to the higher mean firing rates to a female stimulus than to a male, which in turn would lead to a greater absolute variance from trial to trial. To rule out this possibility, we compared the data from sessions where the same stimulus was repeatedly presented (Figures S5A and S5B) to sessions where two different stimuli were presented (Figures 4D and 4E). The firing rate difference for repeated presentations of the same stimulus was markedly different when compared to presentation of different stimuli for females ($p = 0.0208$; Figure S5C) but not so for males ($p = 0.3542$; Figure S5D). Since the F1 versus F2 difference was greater than the F1 versus F1 difference, it appears that the neurons discriminate between two different females and do not vary at random. However, the M1 versus M2 difference was the same as that for M1 versus M1, suggesting that the subject rats do not discriminate between the males.

Responses to Objects in Ventral CA1

In order to determine if the abovementioned responses in the vCA1 were specific to conspecifics, we compared the neurons' responses when objects were presented to the subject rats. Similar to social touch, object touch in general led to an inhibition of vCA1 units (example shown in Figures 5A and 5B; population response indices shown in Figure 5D). Object presence on the other hand resulted in little or no modulation (Figure 5C; unit

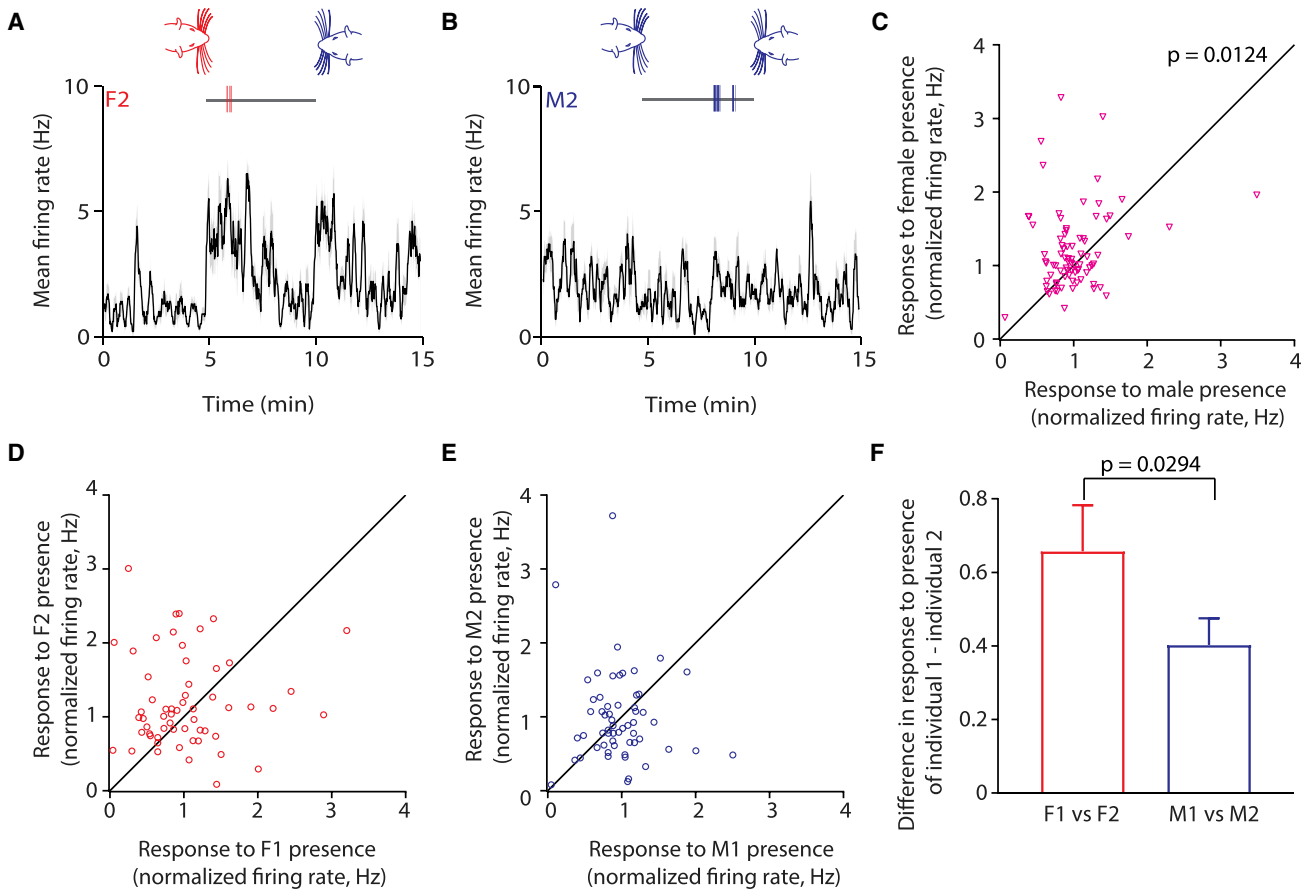

Figure 4. In Males, Ventral CA1 Cells Respond More Strongly to Females Than to Males and Discriminate More Strongly between Females

(A) Example of a vCA1 unit that showed large firing rate modulations when presented with a female conspecific. Facial interactions with this female are indicated by red vertical lines.

(B) The same unit does not show any modulation when exposed to a male conspecific (despite several facial interactions indicated by blue vertical lines).

(C) Scatterplot comparing the response of each vCA1 unit to the presence of female stimuli versus male stimuli (normalized firing rates; p = 0.0124, n = 81, Wilcoxon signed rank test).

(D) Scatterplot comparing the response of vCA1 units to the presence of one individual female versus another (normalized firing rates; F1 versus F2, n = 61).

(E) Scatterplot comparing the response of vCA1 units to the presence of one individual male versus another (normalized firing rates; M1 versus M2, n = 60).

(F) Difference in response between two individuals is significantly greater for females than for males (p = 0.0294, Mann-Whitney test).

shown in Figures 5A and 5B). The object presence population response indices were close to zero and significantly different from object touch (p = 0.0004; Figure 5D). Unlike conspecifics, objects seldom elicited large modulations in vCA1 activity. A univariate plot of the peak z-score reached during individual recording sessions shows few large magnitude z-score excursions when objects were presented (Figure 5E). However, social stimuli frequently elicited significantly larger peak z-score changes (p = 0.0042; Figure 5E). Object presence neither modulated theta activity in the ventral hippocampus (Figure S6A) nor did it lead to a change in the frequency of SWRs when compared to the subject-alone condition (Figure S6B).

Conspecific and Object Presence Responses Differ between Dorsal and Ventral CA1

In light of several studies that showed that dCA1 was only weakly modulated by the presence of conspecifics (Alexander et al., 2016; von Heimendahl et al., 2012; Zynyuk et al., 2012), we were interested in comparing the responses of dCA1 to those of vCA1. To this end, we re-analyzed the behavioral data of our earlier study (von Heimendahl et al., 2012) to identify 976 whisker-to-whisker and 703 snout-to-snout contacts in addition to durations of stimulus presence. This enabled us to compare touch and presence responses in dCA1 (Figure S1L) to those in vCA1 in exactly the same way.

Comparison of firing rates during social presence versus baseline shows several socially responsive (and a few inhibited) units in vCA1 (Figure 6A). However, almost all the dCA1 units were inhibited by social presence (p < 0.0001; Figure 6B). This appears to be in line with our earlier observations (von Heimendahl et al., 2012). Analysis of response indices showed that the vCA1 population consisted of both positively and negatively modulated units (Figure 6C, left). A greater

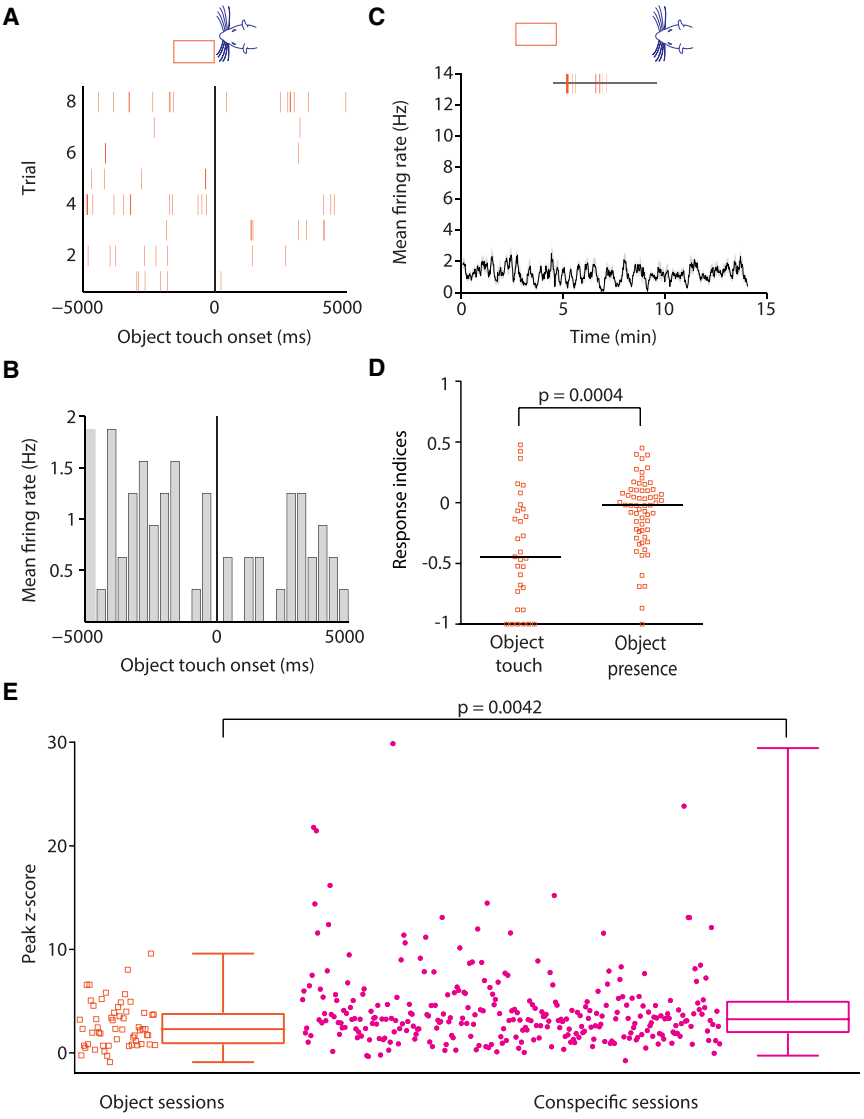

Figure 5. Object Touch Inhibits the Ventral CA1, but Object Presence Has no Effect

(A) Spike rasters for a vCA1 unit showing an inhibitory response when aligned to onset of whisker touch onto an object.

(B) PSTH for unit from (A) showed a decrease in firing rate upon whisker touch (bin size: 400 ms).

(C) Moving average plot of unit from (A) showing little or no modulation due to object presence (indicated by gray horizontal line), despite numerous interactions (indicated by orange vertical lines).

(D) Mean response indices of vCA1 units showing that object touch led to significant inhibition unlike object presence, which elicited little or no modulation ($p = 0.0004$, Mann-Whitney test). Horizontal lines indicate population medians.

(E) Univariate plot of session-wise peak z-scores in vCA1 units. Sessions where objects were present elicit very few large-scale increases (orange open squares, $n = 56$), unlike sessions where social stimuli were presented (magenta filled circles, $n = 306$). Box and whisker plots indicate that object sessions were significantly different from conspecific ones ($p = 0.0042$, Mann-Whitney Test).

fraction of dCA1 units appear to be unmodulated and the rest were almost entirely inhibited (Figure 6C, right). A comparison of the two distributions revealed that they were significantly different ($p = 0.0033$). The ripple activity in the dorsal hippocampus was also reduced due to both conspecific ($p = 0.0006$; Figure S7A) and object presence ($p = 0.0004$; Figure S7B) when compared to subject-alone epochs. Again, this was different from the ventral hippocampus where conspecific (but not object) presence led to an increase in ripple activity (Figure 2, Figure S6B). The vCA1 responses due to conspecific presence were also distinct and very different from those we observed in a subset of CA2 units that we recorded in the course of our experiments. First, almost all CA2 units showed a small but significant increase in their firing rates due to conspecific ($p = 0.0003$; Figure S7C) but not object presence ($p = 0.1688$; Figure S7D). Second, none of the CA2 units showed large-scale modulations characteristic of vCA1. Lastly, the CA2 units did not show any differences that could be attributed to the sex or the individual presented.

Social versus Object Presence: Individual vCA1 (but Not dCA1) Units Discriminate between Social Stimuli and Objects

To study the preference of each neuron, we compared its baseline-normalized firing rate for conspecific presence to that for object presence. The vCA1 neurons as a population showed a greater preference for social stimuli ($p = 0.006$; Figure 6D), while the dCA1 neurons do not appear to discriminate between the two ($p = 0.2752$; Figure 6E). We computed a preference index to quantify each unit's preference for conspecifics versus object stimuli and observed a skew toward social stimuli for vCA1 (Figure 6F, left). The dCA1 population skewed toward objects (Figure 6F, right); and these two distributions are significantly different from each other ($p = 0.0177$).

DISCUSSION

The ability to recognize conspecifics facilitates social interactions that are key to an individual's survival. Physiological evidence has demonstrated the existence of cells selective to specific individuals in humans (Quiroga et al., 2005) and monkeys (Sliwa et al., 2016). In this study, we investigated the physiological responses of ventral hippocampal neurons when awake-behaving rats interacted with conspecifics. We also compared our findings to a previous study (von Heimendahl et al., 2012),

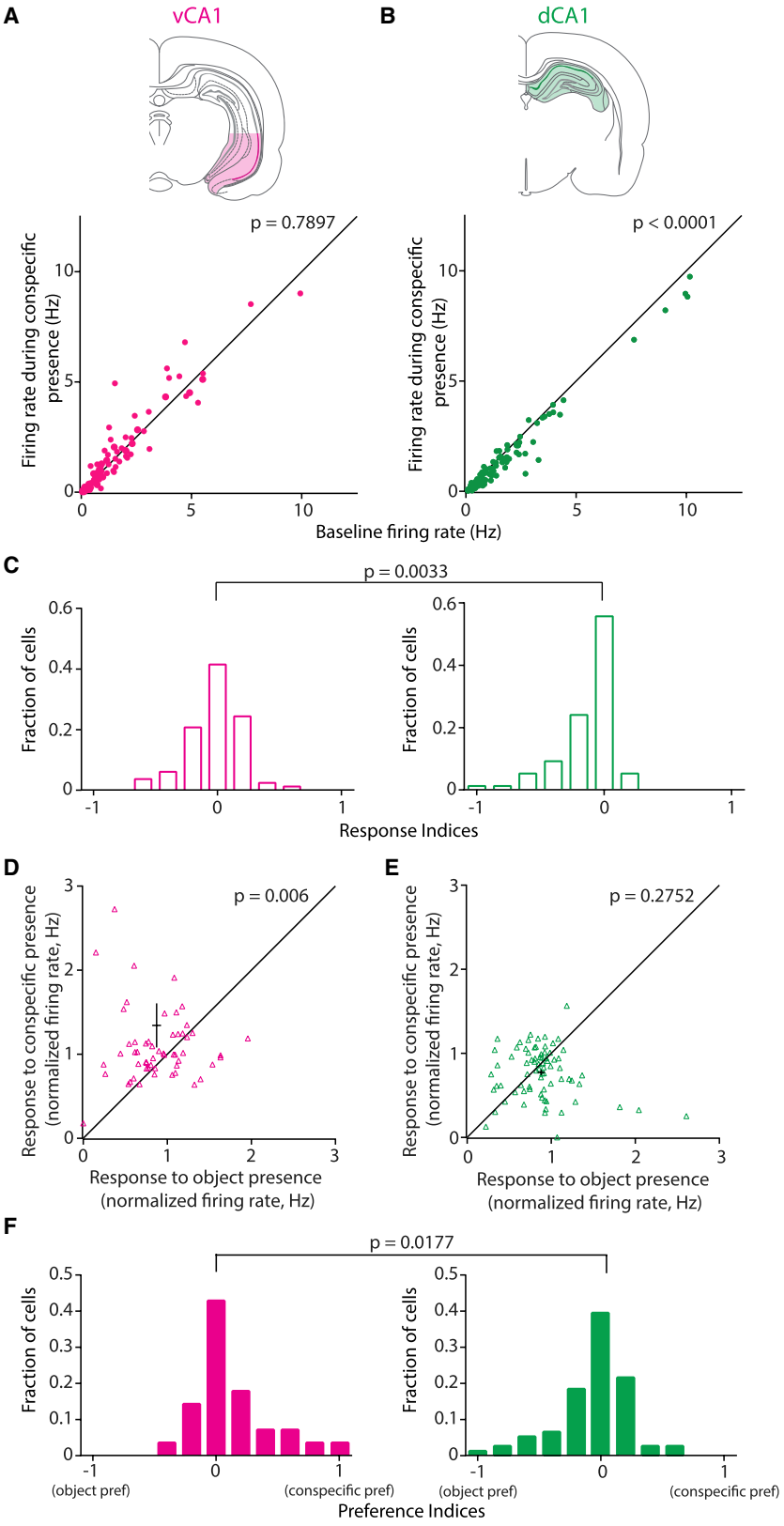

Figure 6. Ventral CA1 (but Not Dorsal CA1) Units Fire Preferentially for Conspecifics over Objects

(A) Scatterplots comparing firing rates of vCA1 units during conspecific presence versus baseline ($p = 0.7897$, $n = 82$, Wilcoxon signed rank test).

(B) Scatterplots comparing firing rates of dCA1 units during conspecific presence versus baseline ($p < 0.0001$, $n = 101$, Wilcoxon signed rank test).

(C) Comparison of distributions of response indices showed that while vCA1 units (left) were both positively and negatively modulated by conspecific presence, dCA1 units (right) were mostly inhibited ($p = 0.0033$, Kolmogorov-Smirnov test).

(D) Scatterplot comparing response of vCA1 units to the presence of conspecifics versus objects (normalized firing rates; $p = 0.006$, $n = 56$, Wilcoxon signed rank test). Population mean ± SEM is indicated in black.

(E) Scatterplot comparing response of dCA1 units to the presence of conspecifics versus objects (normalized firing rates; $p = 0.2752$, $n = 76$, Wilcoxon signed rank test). Population mean ± SEM is indicated in black.

(F) Distribution of conspecific versus object preference indices in vCA1 (left) and dCA1 (right) indicating complete social preference (+1), no preference (0), or complete object preference (−1). vCA1 units are skewed toward conspecifics, while dCA1 units do not discriminate between conspecifics and objects ($p = 0.0177$, Kolmogorov-Smirnov test).

which involved a similar analysis in the dorsal hippocampus. In a population of vCA1 neurons, we observed large modulations by conspecific (but not object) presence. They were repeatable when the same conspecific was presented and differential when different conspecifics were presented. These do not appear to be related to any obvious behavioral, attentional, or spatial contingencies. The vCA1 neurons showed modulation to multisensory inputs and this potentially contributes to their ability to discriminate between the sex and individual presented. Conspecific presence, on the other hand, had little or no effect on dCA1 activity.

Modulation of vCA1 by Conspecific Presence

The most striking feature of our results was the large firing rate modulations in a fraction of vCA1 neurons. At first glance, they did not appear to be linked to facial interactions but to the presence of conspecifics (Figures 1C–1F and 5E) and were almost never observed when object controls were presented (Figure 5E). Little is known about such modulations of activity over extended periods of time. The only report we have come across showed a similar modulation of amygdala neurons when presented with a conspecific (J. O'Keefe, 2012, 8th FENS Forum of Neuroscience, conference). The ventral hippocampus and amygdala have extensive reciprocal projections (Strange et al., 2014) and bidirectional signaling occurs during social interactions (Felix-Ortiz and Tye, 2014). These firing patterns are distinct from those observed in the somatosensory cortex, where responses were tightly correlated to facial touch (Bobrov et al., 2014; Lenschow and Brecht, 2015). Another characteristic feature was that while vCA1 responses were reliably similar when the same conspecific was subject to repeated presentations, the presentation of different conspecifics resulted in differential responses. As a consequence, responses elicited by conspecifics were observed in at least one recording session of a large fraction of vCA1 neurons (54%). Cells that had strong responses during more than one session constituted a smaller fraction (~10%), similar to an earlier report (Okuyama et al., 2016).

We then addressed the behavioral and spatial factors that could confound our observations. The introduction of a salient stimulus such as a conspecific leads to changes in the subject's activity, which in turn would influence speed-modulated hippocampal cells (McFarland et al., 1975). However, we observed no correlation between vCA1 activity and running speeds (Figure S2). As for spatial confounds, we ruled out place cell activity in the gap by analyzing spatial firing rate plots (Figures S3A and S3B). We observed no distinct place field activity, neither when a subject was alone nor after conspecific introduction. The spatial correlations between subject-alone and conspecific-present epochs were low (Figure S3C). Spatial information content (Skaggs et al., 1992) was also low (Figure S3D), and comparable to an earlier report (Keinath et al., 2014). In our hands, vCA1 units that show modulation by conspecific presence have little or no spatial modulation. It must however be noted that the gap paradigm affords minimal mobility and an open-field arena would be more suited to studying the relationship between social and spatial coding. That said, the combined coding of social and spatial signals occurs in the prefrontal cortex (Murugan et al., 2017). The authors have suggested that social information to the prefrontal cortex likely comes from the ventral hippocampus but that remains to be demonstrated (Murugan et al., 2017).

The presence of conspecifics led to only a marginal increase in theta power and that was not different from subject-alone epochs (Figures S4A–S4C). The theta power in itself was weak and not modulated by running speed (Figure S4G). These observations are similar to earlier studies that have reported both weak theta power and a smaller fraction of theta-modulated neurons in the ventral hippocampus (Patel et al., 2012; Royer et al., 2010). The lack of theta modulation by conspecific presence however does not preclude the fact that the ventral hippocampus may still be responding to subtle changes in behavior other than changes in running speed. SWR activity was increased in the ventral hippocampus (Figure 2C), while object presence had no effect (Figure S6B). This may be related to an altered attentional state. SWR activity is associated with reduced inhibition and altered neuromodulatory signals (Colgin, 2016). Pyramidal neuronal activity may increase as a consequence of increased ripple activity. The socially responsive CA2 sub-field (Hitti and Siegelbaum, 2014) triggers SWRs (Oliva et al., 2016). Direct projections from CA2 to the ventral hippocampus exist (Meira et al., 2018; Okuyama et al., 2016) and likely form the basis of the increased SWR activity. While little is known about the role of SWRs in social memory processing, awake SWR activity is involved in the learning, retrieval, and consolidation of spatial memories (Carr et al., 2011; Colgin, 2016). Disruption of awake SWR activity leads to deficits in spatial learning and memory (Jadhav et al., 2012; Nokia et al., 2012).

The modulation of vCA1 units depends on the individual presented and its sex (Figure 4). Also, the ability to discriminate between two individuals of opposite sex is better than the ability to discriminate between two individuals of the same sex. However, it must be borne in mind that that these observations are from male subject rats and with a limited number of stimulus presentations, which are complicated by our experimental design. Interestingly, the responses did not depend on the sexual state of the females presented (Figure S5A). There is extensive literature indicating a sex difference in juvenile rats with regard to social recognition, in the context of vasopressin signaling in the lateral septum (Veenema et al., 2012). Signaling between the lateral septum and ventral hippocampus (e.g., Siegel and Tassoni, 1971) is involved in emotional and feeding behaviors (Calfa et al., 2007; Sweeney and Yang, 2015; Trent and Menard, 2010). The role of the ventral hippocampus-lateral septum circuit in sex discrimination remains to be investigated. While salience could theoretically explain some of our observations, the fact that we observe individual discrimination despite presenting two very salient stimuli suggests that the responses are perhaps not due to salience. Salience (along with novelty and goal information) is encoded by the ventral tegmental area (VTA), with input from the hippocampus (Lisman and Grace, 2005). The ventral hippocampal responses could be attributed to the passage of time, as CA1 activity is known to change over time (Mankin et al., 2012; Manns et al., 2007), and different neuronal firing rates between two stimuli may simply be due to the passage of time. Since we compare the stimulus-evoked activity with baselines in each recording session, we consider this argument as unlikely.

Modulation of vCA1 by Multisensory Inputs

In humans and primates, individual discrimination primarily occurs by facial recognition and the role of visual areas is well documented (Sugita, 2009). "Gnostic cells" in the human medial temporal lobe respond not only to individual faces, but also written and spoken nouns associated with the individual (Quiroga, 2012). Similarly, monkey hippocampal cells code for both facial and vocal identity (Sliwa et al., 2016). The rat somatosensory cortex is capable of discriminating between social and object touch, and also between female and male touch in a manner that is dependent on the sexual state of the female (Bobrov et al., 2014; Lenschow and Brecht, 2015). This led us to investigate if information arising out of facial touch could be transmitted to the ventral hippocampus. Indeed, when we aligned the firing rates of these neurons to the onset of facial touch, nearly a third of the vCA1 units showed significant inhibition to facial and object touch (Figures 3B, 3C, 5A, 5B, and 5D). A smaller fraction (~10%) showed significant excitatory responses suggesting strong modulation by touch. Facial interactions in a gap paradigm are associated with a dramatic increase in ultrasonic vocalizations (Rao et al., 2014). Despite not observing any obvious examples of vCA1 units being responsive to calls (possibly due to low sampling), it does appear that the population is modulated by vocalizations. Similar to the auditory cortex (Rao et al., 2014), vCA1 appears to discriminate between the subject's own calls and stimulus calls (Figures 3D–3F). The exact role played by touch- and call-elicited inhibition remains unclear. Previously, we observed that touch-mediated inhibition modulates the responsiveness of auditory cortex neurons to ultrasonic vocalizations (Rao et al., 2014). In vCA1 (similar to the auditory cortex), this inhibition appears to be mediated by both conspecific and object touch, suggesting that it is a generalized mechanism. Whether multisensory integration mechanisms similar to those in the auditory cortex are also at play in the ventral hippocampus remains to be studied. Another noteworthy aspect of responses to touch and calls in vCA1 is the distinctly delayed time scales, when compared to fast (<100 ms) responses observed in somatosensory (Bobrov et al., 2014; Lenschow and Brecht, 2015) and auditory cortices (Rao et al., 2014), possibly due to indirect inputs via the perirhinal cortex (Burwell, 2000), which has been implicated in individual discrimination (Petrulis and Eichenbaum, 2003). This is suggestive of Brown and Aggleton's dual-process model wherein the perirhinal cortex plays a role in single-item, rapid, familiarity discrimination whereas the hippocampus is involved in slower, multi-item, associational, and recollective aspects of recognition memory (Brown and Aggleton, 2001).

The Role of the Hippocampus in Social Behavior

Scoville and Milner's seminal report was the first to identify the hippocampal formation as being crucial for declarative memories (Scoville and Milner, 1957). The discovery of place cells (O'Keefe and Dostrovsky, 1971) and subsequent studies have demonstrated a role for the hippocampus in spatial navigation. Several (if not all) lesion studies in mice, rats, and cats showed that this area also plays a role in social, maternal, and sexual behaviors (O'Keefe and Nadel, 1978). Subsequently, based on anatomical evidence, it was suggested that the hippocampus is not a unitary structure but in fact is differentiated along its dorsoventral (septotemporal) axis (Moser and Moser, 1998). Not only are there spatially distinct afferents bringing information into dorsal and ventral poles of the hippocampus from sensory cortices (via entorhinal cortex), there are even more striking efferent connections; with the dorsal hippocampus sending projections mostly to the neocortex, while the ventral pole is preferentially connected to subcortical entities such as the amygdala and hypothalamus (van Strien et al., 2009). This difference in functional connectivity has specific effects, with precise lesions of the dorsal (but not the ventral) pole leading to deficits in spatial navigation (Moser et al., 1993). Differences in spatial representations (especially the sizes of place fields) occur along the dorsoventral axis (Jung et al., 1994; Kjelstrup et al., 2008; Maurer et al., 2005; Royer et al., 2010) Ventral lesions however lead to affective deficits (Bannerman et al., 2003; Kjelstrup et al., 2002) and changes in stress responsiveness (Henke, 1990). Septotemporal differences exist in the propagation of theta waves (Patel et al., 2012) and ripples (Patel et al., 2013). Further, the existence of several distinct functional domains along the dorsoventral axis has been bolstered by molecular characterization of hippocampal sub-fields (Cembrowski et al., 2016; Dong et al., 2009; Fanselow and Dong, 2010; Strange et al., 2014).

In our earlier study, we found no evidence for place-independent responses to rats in dCA1 (von Heimendahl et al., 2012). In a concurrently published report using an open field, the presence of a second rat again had little or no effect on the location-specific firing of dCA1 place cells (Zynyuk et al., 2012). This is striking, as local objects modulate place cell activity (Deshmukh and Knierim, 2013). In yet another study, it was shown that dCA1 (used as a control in two different rat strains in two different laboratories) does not undergo global remapping upon presentation of a social stimulus (Alexander et al., 2016). There was no increase in the proportion of dCA1 coding for an individual after familiarization (Okuyama et al., 2016). There appears to be a sufficiently large amount of evidence to suggest that the dorsal hippocampus is minimally involved in the representation of social signals. However, the dorsal hippocampus does appear to be involved in representing the positional information of other conspecifics (Danjo et al., 2018; Omer et al., 2018). On the other hand, recent studies have shown that a dCA2-vCA1-Nac circuit forms the basis for social memory processing (Alexander et al., 2016; Hitti and Siegelbaum, 2014; Meira et al., 2018; Okuyama et al., 2016). In this study, we show that vCA1 activity is modulated by the presence of conspecifics. The cells exhibit sex and individual selectivity and the responses are distinct from those observed in dCA1. Taken together, these data speak for social representations in the ventral hippocampus of the rat.

STAR★METHODS

Detailed methods are provided in the online version of this paper and include the following:

- KEY RESOURCES TABLE
- LEAD CONTACT AND MATERIALS AVAILABILITY
- EXPERIMENTAL MODEL AND SUBJECT DETAILS
- METHOD DETAILS

SUPPLEMENTAL INFORMATION

Supplemental Information can be found online at https://doi.org/10.1016/j.celrep.2019.05.081.

ACKNOWLEDGMENTS

This work was supported by Humboldt Universität zu Berlin, Bernstein Center for Computational Neuroscience Berlin, German Federal Ministry of Education and Research (BMBF, Förderkennzeichen 01GQ1001A), Neurocure, and SFB 1315/1. M.B. was a recipient of the Gottfried Wilhelm Leibniz Prize. We thank U. Schneeweiß, A. Neukirchner, M. Kunert, and J. Diederichs for technical assistance; F. Mielke and D. Spicher for software development; E. Chorev for theta and ripple analyses codes; C. Mende and E. Bobrov for artwork; and J.I. Sanguinetti, S. Ray, K. Hartmann, A. Clemens, E. Chorev, S. Ishiyama, P. Bennett, and members of the Brecht lab for valuable comments.

AUTHOR CONTRIBUTIONS

Conceptualization and Methodology, R.P.R. and M.B.; Investigation, R.P.R. and M.v.H.; Formal Analysis, R.P.R., M.v.H., V.B., and M.B.; Software, M.v.H. and V.B.; Data Curation, R.P.R. and M.v.H.; Writing – Original Draft, R.P.R.; Writing – Review & Editing, R.P.R., M.v.H., V.B., and M.B.; Visualization, R.P.R. and V.B.; Supervision, Project Administration, and Funding Acquisition, M.B.

DECLARATION OF INTERESTS

The authors declare no competing interests.

Received: December 3, 2018
Revised: April 5, 2019
Accepted: May 21, 2019
Published: June 18, 2019

REFERENCES

Alexander, G.M., Farris, S., Pirone, J.R., Zheng, C., Colgin, L.L., and Dudek, S.M. (2016). Social and novel contexts modify hippocampal CA2 representations of space. Nat. Commun. *7*, 10300.

Anderson, D.J. (2016). Circuit modules linking internal states and social behaviour in flies and mice. Nat. Rev. Neurosci. *17*, 692–704.

Bannerman, D.M., Lemaire, M., Beggs, S., Rawlins, J.N.P., and Iversen, S.D. (2001). Cytotoxic lesions of the hippocampus increase social investigation but do not impair social-recognition memory. Exp. Brain Res. *138*, 100–109.

Bannerman, D.M., Grubb, M., Deacon, R.M.J., Yee, B.K., Feldon, J., and Rawlins, J.N.P. (2003). Ventral hippocampal lesions affect anxiety but not spatial learning. Behav. Brain Res. *139*, 197–213.

Barnett, S.A. (1958). An analysis of social behaviour in wild rats. Proc. Zool. Soc. Lond. *130*, 107–152.

Becker, A., Grecksch, G., Bernstein, H.-G., Höllt, V., and Bogerts, B. (1999). Social behaviour in rats lesioned with ibotenic acid in the hippocampus: quantitative and qualitative analysis. Psychopharmacology (Berl.) *144*, 333–338.

Bobrov, E. (2014). Rat social touch. (Humboldt-Universität zu Berlin, Mathematisch-Naturwissenschaftliche Fakultät I), PhD dissertation.

Bobrov, E., Wolfe, J., Rao, R.P., and Brecht, M. (2014). The representation of social facial touch in rat barrel cortex. Curr. Biol. *24*, 109–115.

Brown, M.W., and Aggleton, J.P. (2001). Recognition memory: what are the roles of the perirhinal cortex and hippocampus? Nat. Rev. Neurosci. *2*, 51–61.

Burwell, R.D. (2000). The parahippocampal region: corticocortical connectivity. Ann. N Y Acad. Sci. *911*, 25–42.

Calfa, G., Bussolino, D., and Molina, V.A. (2007). Involvement of the lateral septum and the ventral Hippocampus in the emotional sequelae induced by social defeat: role of glucocorticoid receptors. Behav. Brain Res. *181*, 23–34.

Carr, M.F., Jadhav, S.P., and Frank, L.M. (2011). Hippocampal replay in the awake state: a potential substrate for memory consolidation and retrieval. Nat. Neurosci. *14*, 147–153.

Cembrowski, M.S., Bachman, J.L., Wang, L., Sugino, K., Shields, B.C., and Spruston, N. (2016). Spatial Gene-Expression Gradients Underlie Prominent Heterogeneity of CA1 Pyramidal Neurons. Neuron *89*, 351–368.

Chiang, M.-C., Huang, A.J.Y., Wintzer, M.E., Ohshima, T., and McHugh, T.J. (2018). A role for CA3 in social recognition memory. Behav. Brain Res. *354*, 22–30.

Colgin, L.L. (2016). Rhythms of the hippocampal network. Nat. Rev. Neurosci. *17*, 239–249.

Daenen, E.W.P.M., Wolterink, G., Gerrits, M.A.F.M., and Van Ree, J.M. (2002). The effects of neonatal lesions in the amygdala or ventral hippocampus on social behaviour later in life. Behav. Brain Res. *136*, 571–582.

Danjo, T., Toyoizumi, T., and Fujisawa, S. (2018). Spatial representations of self and other in the hippocampus. Science *359*, 213–218.

Deshmukh, S.S., and Knierim, J.J. (2013). Influence of local objects on hippocampal representations: Landmark vectors and memory. Hippocampus *23*, 253–267.

Dong, H.-W., Swanson, L.W., Chen, L., Fanselow, M.S., and Toga, A.W. (2009). Genomic-anatomic evidence for distinct functional domains in hippocampal field CA1. Proc. Natl. Acad. Sci. USA *106*, 11794–11799.

Dulac, C., O'Connell, L.A., and Wu, Z. (2014). Neural control of maternal and paternal behaviors. Science *345*, 765–770.

Fanselow, M.S., and Dong, H.-W. (2010). Are the dorsal and ventral hippocampus functionally distinct structures? Neuron *65*, 7–19.

Feinberg, L.M., Allen, T.A., Ly, D., and Fortin, N.J. (2012). Recognition memory for social and non-social odors: differential effects of neurotoxic lesions to the hippocampus and perirhinal cortex. Neurobiol. Learn. Mem. *97*, 7–16.

Felix-Ortiz, A.C., and Tye, K.M. (2014). Amygdala inputs to the ventral hippocampus bidirectionally modulate social behavior. J. Neurosci. *34*, 586–595.

Gheusi, G., Goodall, G., and Dantzer, R. (1997). Individually distinctive odours represent individual conspecifics in rats. Anim. Behav. *53*, 935–944.

Henke, P.G. (1990). Hippocampal pathway to the amygdala and stress ulcer development. Brain Res. Bull. *25*, 691–695.

Hitti, F.L., and Siegelbaum, S.A. (2014). The hippocampal CA2 region is essential for social memory. Nature *508*, 88–92.

Husted, J.R., and McKenna, F.S. (1966). The use of rats as discriminative stimuli. J. Exp. Anal. Behav. *9*, 677–679.

Jadhav, S.P., Kemere, C., German, P.W., and Frank, L.M. (2012). Awake hippocampal sharp-wave ripples support spatial memory. Science *336*, 1454–1458.

Johnston, R.E., and Jernigan, P. (1994). Golden hamsters recognize individuals, not just individual scents. Anim. Behav. *48*, 129–136.

Jung, M.W., Wiener, S.I., and McNaughton, B.L. (1994). Comparison of spatial firing characteristics of units in dorsal and ventral hippocampus of the rat. J. Neurosci. *14*, 7347–7356.

Keinath, A.T., Wang, M.E., Wann, E.G., Yuan, R.K., Dudman, J.T., and Muzzio, I.A. (2014). Precise spatial coding is preserved along the longitudinal hippocampal axis. Hippocampus *24*, 1533–1548.

Kjelstrup, K.B., Solstad, T., Brun, V.H., Hafting, T., Leutgeb, S., Witter, M.P., Moser, E.I., and Moser, M.-B. (2008). Finite scale of spatial representation in the hippocampus. Science *321*, 140–143.

Kjelstrup, K.G., Tuvnes, F.A., Steffenach, H.-A., Murison, R., Moser, E.I., and Moser, M.-B. (2002). Reduced fear expression after lesions of the ventral hippocampus. Proc. Natl. Acad. Sci. USA *99*, 10825–10830.

Kogan, J.H., Frankland, P.W., and Silva, A.J. (2000). Long-term memory underlying hippocampus-dependent social recognition in mice. Hippocampus *10*, 47–56.

Lai, W.-S., Ramiro, L.-L.R., Yu, H.A., and Johnston, R.E. (2005). Recognition of familiar individuals in golden hamsters: a new method and functional neuroanatomy. J. Neurosci. *25*, 11239–11247.

Lenschow, C., and Brecht, M. (2015). Barrel cortex membrane potential dynamics in social touch. Neuron *85*, 718–725.

Lin, Y.-T., Hsieh, T.-Y., Tsai, T.-C., Chen, C.-C., Huang, C.-C., and Hsu, K.-S. (2018). Conditional Deletion of Hippocampal CA2/CA3a Oxytocin Receptors Impairs the Persistence of Long-Term Social Recognition Memory in Mice. J. Neurosci. *38*, 1218–1231.

Lisman, J.E., and Grace, A.A. (2005). The hippocampal-VTA loop: controlling the entry of information into long-term memory. Neuron *46*, 703–713.

Mankin, E.A., Sparks, F.T., Slayyeh, B., Sutherland, R.J., Leutgeb, S., and Leutgeb, J.K. (2012). Neuronal code for extended time in the hippocampus. Proc. Natl. Acad. Sci. USA *109*, 19462–19467.

Manns, J.R., Howard, M.W., and Eichenbaum, H. (2007). Gradual changes in hippocampal activity support remembering the order of events. Neuron *56*, 530–540.

Maurer, A.P., Vanrhoads, S.R., Sutherland, G.R., Lipa, P., and McNaughton, B.L. (2005). Self-motion and the origin of differential spatial scaling along the septo-temporal axis of the hippocampus. Hippocampus *15*, 841–852.

McFarland, W.L., Teitelbaum, H., and Hedges, E.K. (1975). Relationship between hippocampal theta activity and running speed in the rat. J. Comp. Physiol. Psychol. *88*, 324–328.

Meira, T., Leroy, F., Buss, E.W., Oliva, A., Park, J., and Siegelbaum, S.A. (2018). A hippocampal circuit linking dorsal CA2 to ventral CA1 critical for social memory dynamics. Nat. Commun. *9*, 4163.

Moles, A., Costantini, F., Garbugino, L., Zanettini, C., and D'Amato, F.R. (2007). Ultrasonic vocalizations emitted during dyadic interactions in female mice: a possible index of sociability? Behav. Brain Res. *182*, 223–230.

Moser, E., Moser, M.B., and Andersen, P. (1993). Spatial learning impairment parallels the magnitude of dorsal hippocampal lesions, but is hardly present following ventral lesions. J. Neurosci. *13*, 3916–3925.

Moser, M.-B., and Moser, E.I. (1998). Functional differentiation in the hippocampus. Hippocampus *8*, 608–619.

Murugan, M., Jang, H.J., Park, M., Miller, E.M., Cox, J., Taliaferro, J.P., Parker, N.F., Bhave, V., Hur, H., Liang, Y., et al. (2017). Combined Social and Spatial Coding in a Descending Projection from the Prefrontal Cortex. Cell *171*, 1663–1677.e16.

Nokia, M.S., Mikkonen, J.E., Penttonen, M., and Wikgren, J. (2012). Disrupting neural activity related to awake-state sharp wave-ripple complexes prevents hippocampal learning. Front. Behav. Neurosci. *6*, 84.

O'Keefe, J., and Dostrovsky, J. (1971). The hippocampus as a spatial map. Preliminary evidence from unit activity in the freely-moving rat. Brain Res. *34*, 171–175.

O'Keefe, J., and Nadel, L. (1978). The Hippocampus as a Cognitive Map (Clarendon Press).

Okuyama, T., Kitamura, T., Roy, D.S., Itohara, S., and Tonegawa, S. (2016). Ventral CA1 neurons store social memory. Science *353*, 1536–1541.

Oliva, A., Fernández-Ruiz, A., Buzsáki, G., and Berényi, A. (2016). Role of Hippocampal CA2 Region in Triggering Sharp-Wave Ripples. Neuron *91*, 1342–1355.

Omer, D.B., Maimon, S.R., Las, L., and Ulanovsky, N. (2018). Social place-cells in the bat hippocampus. Science *359*, 218–224.

Patel, J., Fujisawa, S., Berényi, A., Royer, S., and Buzsáki, G. (2012). Traveling theta waves along the entire septotemporal axis of the hippocampus. Neuron *75*, 410–417.

Patel, J., Schomburg, E.W., Berényi, A., Fujisawa, S., and Buzsáki, G. (2013). Local generation and propagation of ripples along the septotemporal axis of the hippocampus. J. Neurosci. *33*, 17029–17041.

Petrulis, A. (2009). Neural mechanisms of individual and sexual recognition in Syrian hamsters (*Mesocricetus auratus*). Behav. Brain Res. *200*, 260–267.

Petrulis, A., and Eichenbaum, H. (2003). The perirhinal-entorhinal cortex, but not the hippocampus, is critical for expression of individual recognition in the context of the Coolidge effect. Neuroscience *122*, 599–607.

Popik, P., Vetulani, J., Bisaga, A., and van Ree, J.M. (1991). Recognition cue in the rat's social memory paradigm. J. Basic Clin. Physiol. Pharmacol. *2*, 315–327.

Poucet, B., Thinus-Blanc, C., and Muller, R.U. (1994). Place cells in the ventral hippocampus of rats. Neuroreport *5*, 2045–2048.

Quian Quiroga, R., Kraskov, A., Koch, C., and Fried, I. (2009). Explicit encoding of multimodal percepts by single neurons in the human brain. Curr. Biol. *19*, 1308–1313.

Quiroga, R.Q. (2012). Concept cells: the building blocks of declarative memory functions. Nat. Rev. Neurosci. *13*, 587–597.

Quiroga, R.Q., Reddy, L., Kreiman, G., Koch, C., and Fried, I. (2005). Invariant visual representation by single neurons in the human brain. Nature *435*, 1102–1107.

Raam, T., McAvoy, K.M., Besnard, A., Veenema, A.H., and Sahay, A. (2017). Hippocampal oxytocin receptors are necessary for discrimination of social stimuli. Nat. Commun. *8*, 2001.

Rao, R.P., Mielke, F., Bobrov, E., and Brecht, M. (2014). Vocalization-whisking coordination and multisensory integration of social signals in rat auditory cortex. eLife *3*, e03185.

Royer, S., Sirota, A., Patel, J., and Buzsáki, G. (2010). Distinct representations and theta dynamics in dorsal and ventral hippocampus. J. Neurosci. *30*, 1777–1787.

Sams-Dodd, F., Lipska, B.K., and Weinberger, D.R. (1997). Neonatal lesions of the rat ventral hippocampus result in hyperlocomotion and deficits in social behaviour in adulthood. Psychopharmacology (Berl.) *132*, 303–310.

Sawyer, T.F., Hengehold, A.K., and Perez, W.A. (1984). Chemosensory and hormonal mediation of social memory in male rats. Behav. Neurosci. *98*, 908–913.

Schmitzer-Torbert, N., Jackson, J., Henze, D., Harris, K., and Redish, A.D. (2005). Quantitative measures of cluster quality for use in extracellular recordings. Neuroscience *131*, 1–11.

Scott, J.P. (1966). Agonistic behavior of mice and rats: a review. Am. Zool. *6*, 683–701.

Scoville, W.B., and Milner, B. (1957). Loss of recent memory after bilateral hippocampal lesions. J. Neurol. Neurosurg. Psychiatry *20*, 11–21.

Siegel, A., and Tassoni, J.P. (1971). Differential efferent projections of the lateral and medial septal nuclei to the hippocampus in the cat. Brain Behav. Evol. *4*, 201–219.

Skaggs, W.E., McNaughton, B.L., Gothard, K.M., and Markus, E.J. (1992). An Information-theoretic Approach to Deciphering the Hippocampal Code. In Proceedings of the 5th International Conference on Neural Information Processing Systems (NIPS'92) (Morgan Kaufmann Publishers), pp. 1030–1037.

Sliwa, J., Planté, A., Duhamel, J.-R., and Wirth, S. (2016). Independent Neuronal Representation of Facial and Vocal Identity in the Monkey Hippocampus and Inferotemporal Cortex. Cereb. Cortex *26*, 950–966.

Smith, A.S., Williams Avram, S.K., Cymerblit-Sabba, A., Song, J., and Young, W.S. (2016). Targeted activation of the hippocampal CA2 area strongly enhances social memory. Mol. Psychiatry *21*, 1137–1144.

Squires, A.S., Peddle, R., Milway, S.J., and Harley, C.W. (2006). Cytotoxic lesions of the hippocampus do not impair social recognition memory in socially housed rats. Neurobiol. Learn. Mem. *85*, 95–101.

Stockwell, R.G., Mansinha, L., and Lowe, R.P. (1996). Localization of the complex spectrum: the S transform. IEEE Trans. Signal Process. *44*, 998–1001.

Strange, B.A., Witter, M.P., Lein, E.S., and Moser, E.I. (2014). Functional organization of the hippocampal longitudinal axis. Nat. Rev. Neurosci. *15*, 655–669.

Sugita, Y. (2009). Innate face processing. Curr. Opin. Neurobiol. *19*, 39–44.

Sweeney, P., and Yang, Y. (2015). An excitatory ventral hippocampus to lateral septum circuit that suppresses feeding. Nat. Commun. *6*, 10188.

Thor, D.H., and Holloway, W.R. (1982). Social memory of the male laboratory rat. J. Comp. Physiol. Psychol. *96*, 1000–1006.

Trent, N.L., and Menard, J.L. (2010). The ventral hippocampus and the lateral septum work in tandem to regulate rats' open-arm exploration in the elevated plus-maze. Physiol. Behav. *101*, 141–152.

Uekita, T., and Okanoya, K. (2011). Hippocampus lesions induced deficits in social and spatial recognition in Octodon degus. Behav. Brain Res. *219*, 302–309.

van Strien, N.M., Cappaert, N.L.M., and Witter, M.P. (2009). The anatomy of memory: an interactive overview of the parahippocampal-hippocampal network. Nat. Rev. Neurosci. *10*, 272–282.

Veenema, A.H., Bredewold, R., and De Vries, G.J. (2012). Vasopressin regulates social recognition in juvenile and adult rats of both sexes, but in sex- and age-specific ways. Horm. Behav. *61*, 50–56.

von Heimendahl, M., Rao, R.P., and Brecht, M. (2012). Weak and nondiscriminative responses to conspecifics in the rat hippocampus. J. Neurosci. *32*, 2129–2141.

Wolfe, J., Mende, C., and Brecht, M. (2011). Social facial touch in rats. Behav. Neurosci. *125*, 900–910.

Zola-Morgan, S., Squire, L.R., and Amaral, D.G. (1986). Human amnesia and the medial temporal region: enduring memory impairment following a bilateral lesion limited to field CA1 of the hippocampus. J. Neurosci. *6*, 2950–2967.

Zynyuk, L., Huxter, J., Muller, R.U., and Fox, S.E. (2012). The presence of a second rat has only subtle effects on the location-specific firing of hippocampal place cells. Hippocampus *22*, 1405–1416.

STAR★METHODS

KEY RESOURCES TABLE

REAGENT or RESOURCE	SOURCE	IDENTIFIER
Experimental Models: Organisms/Strains		
Rat (Wistar)	Harlan, Janvier Labs	N/A
Software and Algorithms:		
Avisoft Recorder	Avisoft Bioacoustics	https://www.avisoft.com/
MATLAB	Mathworks	https://de.mathworks.com/
Neurolucida	MBF Biosciences	https://www.mbfbioscience.com/
Prism	GraphPad	https://www.graphpad.com/

LEAD CONTACT AND MATERIALS AVAILABILITY

Further information and requests for resources and reagents should be directed to and will be fulfilled by the Lead Contact, Michael Brecht (michael.brecht@bccn-berlin.de).

EXPERIMENTAL MODEL AND SUBJECT DETAILS

Wistar rats (45-60 days old, males and females) were sourced from either Harlan (Eystrup, Germany) or Janvier Labs (Le Genest-Saint-Isle, France). Animals were housed under inverted dark/light cycles (12:12 h) in groups of 2-3 (except for implanted rats, which were housed singly) with *ad libitum* access to food and water. All experimental procedures were performed in accordance to German regulations on animal welfare (Permit Nos. G0259/09 and G0193/14). After a weeklong post shipment recovery, rats were handled for 2-3 days and subsequently habituated to the setup for 3-4 days. Habituation involved the placement of animals on both platforms of the setup (details below) for 10-15 min and allowing them to explore. The animals often spontaneously indulged in facial interactions (details below) that contributed to the familiarization of other conspecifics and object controls. This was done to avoid confounds due to novelty. Neuronal data was acquired from male subject rats.

METHOD DETAILS

Behavioral Paradigm

The gap paradigm (Bobrov et al., 2014; Rao et al., 2014; von Heimendahl et al., 2012; Wolfe et al., 2011) consists of two elevated platforms (24 × 29.5 cm) separated by a gap (~20 cm; Figure 1A). Rats when placed on the platforms exhibit spontaneous facial interactions that involve extensive whisker and snout contacts. Experiments were conducted under infrared illumination (ABUS, Wetter, Germany). An overhead low speed camera (30 Hz) was used to record behavior. Ultrasonic vocalizations were acquired using 4 condenser ultrasound microphones (Avisoft Bioacoustics, Berlin, Germany) placed under the platforms.

For each recording session, the subject (implanted) rat was alone on the setup (5 min, initial baseline), following which stimulus rats/objects were placed on the opposite platform (5 min, Stimulus present) during which the facial interactions occurred. Subsequently, the stimulus was removed and the subject rat left alone for another 5 min (post-stimulus baseline). In a small subset of experiments, the sessions were ~10 min long (3 min each for initial and post-stimulus baselines, and when stimulus was introduced). On a typical recording day, 5-8 such recording sessions were conducted with various combinations of stimuli presented in a pseudo-random order. The number of sessions was contingent on the subject rat showing approach/exploratory behaviors when the stimuli were presented. The stimuli included age matched conspecifics (females and males) and object controls. Objects were common laboratory equipment such as glove boxes, test tube stands, Styrofoam blocks etc. These stimuli were presented individually. In a small subset of experiments, stimuli were presented more than once to check for the reproducibility of the responses. Foam mats used to line the stimulus platform were changed between sessions to minimize olfactory cues.

Offline video analyses were performed to score for the following behavioral events: whisker overlap onset (Figure S1A, top), snout touch onset (Figure S1A, bottom), snout touch offset, whisker overlap offset, introduction and removal of stimulus from setup. In all, 5.05 million frames were scored to identify 1156 whisker-to-whisker and 858 snout-to-snout contacts. Similar scoring of behavioral events was done for the data acquired while recording from dCA1 (von Heimendahl et al., 2012). Here, 1.17 million frames were analyzed to identify 976 whisker-to-whisker and 703 snout-to-snout contacts.

Electrophysiology

Chronically implanted microdrives (Harlan 8-drive, Neuralynx, Bozeman, MT, USA) consisting of 8 independently movable tetrodes were used to acquire neuronal data from male subject rats (n = 4 for vCA1 recordings and n = 6 for dCA1 recordings), as described elsewhere (Rao et al., 2014; von Heimendahl et al., 2012). Briefly, 17.5 μm diameter tetrodes were fashioned out of platinum-iridium wire (California Fine Wire Company, Grover Beach CA, USA) and were platinum-plated (resistance: 250-300 kΩ, nanoZ, Neuralynx, Bozeman, MT, USA). After implanting and lesioning, ventral hippocampal recording sites (Figure S1B) were assigned to the following bregma locations: −4.68 to −7.08 mm AP; 6.5 to 7.00 mm ML. Microdrives were implanted under ketamine (100 mg/kg body wt)/xylazine (7.5 mg/kg body wt) anesthesia while maintaining body temperature with a heating pad (Stoelting, Wood Dale, IL, USA). After head fixation on stereotactic apparatus (Narashige Scientific Instrument Lab, Tokyo, Japan), the skull surface was treated with UV-activated etchant/glue (Optibond All-In-One, Kerr Italia, Salerno, Italy) and a layer of UV-activated glue to facilitate anchoring of dental cement (Charisma, Heraeus, Hanau, Germany). Gold-plated screws were used for grounding. The microdrive was positioned over the craniotomy, flooded with 1% agarose and secured with dental cement (Paladur, Heraeus Kulzer, Hanau, Germany).

Tetrodes were lowered into the brain and hippocampal recordings typically began 4-6 days after surgery. Tetrodes were advanced by a minimum of 80 μm between recording days. After passing through unity-gain headstage, signals were transmitted to an amplifier (Digital Lynx, Neuralynx, Bozeman, MT, USA). Spike signals were amplified (10x), digitized (at 32 kHz) and bandpass filtered between 600 Hz and 6000 Hz. Events that crossed a user-set threshold were recorded for 1 ms (250 μs before and 750 μs after voltage peak, Figure S1C). For electrode location analysis, rats were anaesthetized and electrolytic lesions (Figure 1B) were performed (10 μA negative current, 10 s, nanoZ, Neuralynx, Bozeman, MT, USA). The rats were perfused and coronal sections (150 μm) of the brains were stained for cytochrome oxidase. Recording depths (determined by number of microdrive turns) were used to identify exact recording sites (Figures S1G–S1K) after accounting for shrinkage during tissue processing (Neurolucida, MBF Bioscience, Williston, VT, USA).

Spike Sorting, Clustering, Cell-Type Classification, and LFP and SWR Analysis

Spike sorting and clustering was also performed as described earlier (Rao et al., 2014). Briefly, amplitude and principal components were used for offline spike sorting (KlustaKwik, KD Harris, Rutgers University, Newark, NJ, USA). Manual correction and refinement was performed (MClust, AD Redish, University of Minnesota, Minneapolis, MN, USA) using MATLAB (MathWorks, Natick, MA, USA). Spike features (energy and first derivative of energy) were used for separation. Inclusion criteria for single units were determined by refractory period, separation quality and stability. Single units were indicated by inter-spike interval histograms with minimal (< 5%) or no contamination in the first two milliseconds bins. Criteria for separation quality was determined by L-ratio (< 0.2) and Isolation Distance (> 15; Schmitzer-Torbert et al., 2005). A total of 116 vCA1 units passed these criteria and were acquired from 4 subject rats (the distribution in each being: 13, 36, 20 and 47 units). Stability of the units was quantified as described earlier (Rao et al., 2014). Spike shapes were used to classify units as putative regular spiking (RS) or fast spiking (FS) neurons. Two features, post trough depth/peak height and time of spike end showed bi-modal distributions when tested on the dataset (arbitrary units on axes indicate relative magnitudes of features compared to the smallest data point; therefore negative values). k-means clustering with two clusters for all units using these features resulted in well separated populations (indicated by dotted line, Figure S1D). Spikes from these two populations resulted in well-defined average spike shapes (Figure S1E) and distinct firing rates (Figure S1F). FS neurons were excluded from analysis. For LFP analysis, the continuously acquired neuronal data was band pass filtered (0 – 9000 Hz) and saved. Custom MATLAB code (kindly provided by F Mielke) was used to generate spectrograms and analyse LFP (using Stockwell Transform as described elsewhere; Stockwell et al., 1996). Time averaged power was computed over the entire duration of stimulus presence and compared with the subject alone epochs. Power during touch episodes was compared to episodes of similar length that occurred 10 s before. In case of another touch episode overlapping at this instance, the baseline episode was again shifted by another 10 s. Custom MATLAB code (kindly provided by E Chorev) was used to detect SWRs. The signal was first low-pass filtered for frequencies below 500 Hz. The hippocampal ripples were isolated after applying a band-pass filter (140-200 Hz). Signal envelope was computed by using the magnitude of the analytical signal computed by the Hilbert transformation. A threshold of > 5 SD was applied on the envelope and epochs that exceeded that threshold were plotted. LFP power and ripple frequency correlations versus running speed were performed for second-to-second data.

Moving Average Plots

Moving average plots were generated using a boxcar function with bin size of 1000 ms and a sliding window of 10000 ms.

Spatial Analysis

In order to extract position data (animal head, platform & gap position) from low-speed videos, we developed custom tracking software based on C++ library OpenCV [74]. After extraction, position data was used for subsequent analysis. For figure generation, we extended a set of custom MATLAB scripts developed earlier (von Heimendahl et al., 2012). Initially, we queried spike times, position data and session-specific metadata. The metadata was used to identify different phases of the experiment (for example, baseline periods or presence of stimulus animals), as well as the identity and other related information of the rats present. After concatenating head positions and spike times from multiple recordings, we discretized the setup into bins of 5 pixels x 5 pixels (1 cm corresponds to 12.5 pixels) and calculated pooled occupancy z for the three experiment phases (initial baseline period, post-stimulus baseline and stimulus presence), as described in detail earlier (von Heimendahl et al., 2012). Auto scaled and rescaled spatial firing rate plots were

generated after incorporating a 1 cm/s speed filter to exclude periods of inactivity. Spatial correlations (r) were calculated on pooled and normalized data from subject alone and stimulus present conditions as described earlier (Alexander et al., 2016). Running speed information was also extracted from tracked head positions, and correlation was calculated for running speed versus firing rate over time (second-to-second comparisons). Spatial information content was computed as described earlier (Skaggs et al., 1992).

Analysis of Presence Responses

In order to determine the significance at the single cell level due to stimulus presence, we adopted a z-score criteria previously reported for monkey face and voice identity cells (Sliwa et al., 2016). Units were considered strongly modulated, if their firing rate during stimulus presentation was at least 4 standard deviations greater than the mean firing rate during the corresponding subject alone epoch (a combination of the initial and end baseline periods). A separate subset of units that showed weaker modulation (< 4 but > 3 standard deviations above mean of initial baseline) was also identified. An important reason for setting these criteria was to control for the difference in the number of presentations of social and object stimuli. Peak and median z-scores were used to characterize the range of firing rate modulations during stimulus presentation.

For conspecific presence, firing rate was defined as mean firing rate during the stimulus present epoch. Similarly, sessions where objects were presented resulted in the object presence firing rates. It must be borne in mind that averaging across the 5 min period leads to an underestimation of firing rates due to stimulus presence. The baseline corresponded to the mean firing rate when the subject was alone. The presence response index was calculated as: Response Index $_{\text{Presence}}$ = (*in* - *out*)/(*in* + *out*), where in and out are the mean firing rates during presence of a stimulus and baselines, respectively. The distribution of response indices was performed by routine frequency distribution analysis with a fixed bin size (0.2).

To compute the response to females versus males, normalized firing rates were averaged over all sessions where either female or male conspecifics were presented. For individual firing rate comparisons, normalized firing rate of one individual (say female 1, F1) was compared to response elicited by another individual within the same sex (female 2, F2). To compare a unit's preference for social versus object stimuli, we computed an index as follows: Preference Index $_{\text{Social versus Object}}$ = Firing rate $_{\text{Social Presence}}$ - Firing rate $_{\text{Object Presence}}$/Firing rate $_{\text{Social Presence}}$ + Firing rate $_{\text{Object Presence}}$. A unit that completely preferred social stimuli would get a score of +1, a unit which fired only for object stimuli would get a score of −1, and a unit with no preference for either would get a score of 0.

Analysis of Touch Responses

For whisker touch events, mean firing rate during all interactions with an interaction partner was computed. The mean firing rate after removing all instances of facial touch was taken as baseline for each single unit. The touch response index was calculated as follows: Response Index $_{\text{Touch}}$ = (in − out)/(in + out), where in and out are mean firing rates during facial touch and baseline, respectively. In order to determine the statistical significance of these touch events, we used a permutation test, as described earlier (Bobrov, 2014). In brief, durations in a particular recording session as long as durations of touch episodes but at random positions outside of the touch episodes were selected. The firing rates during the matched baselines were computed and this was repeated 1000 times. The distribution of these baseline rates was normalized (by mean) and similarly, the firing rates during touch were also normalized. Following this, the rank of the normalized firing rate during touch within the normalized distribution of baseline firing rates was computed.

Analysis of USV Responses

A total of 12,151 ultrasonic vocalizations from 31 sessions were manually identified as described earlier (Rao et al., 2014). The neuronal responses were computed with reference to the onset of each call and a 250 ms response window. The baseline was computed from a time window of the same length as each call, but shifted to 10 s away from call onset. In the event of another call present at this location, the time window was shifted again.

Estrous Staging

At the end of each experimental day's recordings, vaginal smears were obtained from all the female stimulus rats and subjected to routine hematoxylin-eosin staining. Estrous stages were assigned after microscopic examination of the smears.

QUANTIFICATION AND STATISTICAL ANALYSIS

Data was analyzed using Prism 7 (GraphPad Software Inc., La Jolla, CA, USA) or MATLAB (MathWorks, Natick, MA, USA) and is presented as mean ± SEM unless stated otherwise. Neuronal data was acquired from 4 male subject rats. The number of cells/recording sessions (n) analyzed for each condition is indicated in the figure legends. Since most of the data was not normally distributed (tested by D'Agostino & Pearson omnibus normality test), differences between groups were tested with Wilcoxon signed-rank test for paired data and Mann-Whitney U test for unpaired data. Comparison of distributions was performed by Kolmogorov-Smirnov test. Correlations were analyzed using Spearmann's correlation coefficient.